ACS APPLIED MATERIALS & INTERFACES

Research Article

www.acsami.org

Detection and Identification of Cu^{2+} and Hg^{2+} Based on the Cross-reactive Fluorescence Responses of a Dansyl-Functionalized Film in Different Solvents

Yuan Cao, Liping Ding,* Shihuai Wang, Yuan Liu, Junmei Fan, Wenting Hu, Ping Liu, and Yu Fang*

Key Laboratory of Applied Surface and Colloid Chemistry of Ministry of Education, School of Chemistry and Chemical Engineering, Shaanxi Normal University, Xi'an 710062, China

Supporting Information

ABSTRACT: A dansyl-functionalized fluorescent film sensor was specially designed and prepared by assembling dansyl on a glass plate surface via a long flexible spacer containing oligo(oxyethylene) and amine units. The chemical attachment of dansyl moieties on the surface was verified by contact angle, XPS, and fluorescence measurements. Solvent effect examination revealed that the polarity-sensitivity was retained for the surface-confined dansyl moieties. Fluorescence quenching studies in water declared that the dansyl-functionalized SAM possesses a higher sensitivity towards Hg^{2+} and Cu^{2+} than the other tested divalent metal ions including Zn^{2+}, Cd^{2+}, Co^{2+}, and Pb^{2+}. Further measurements of the fluorescence responses of the film towards Cu^{2+} and Hg^{2+} in three solvents including water, acetonitrile, and THF evidenced that the present film exhibits cross-reactive responses to these two metal ions. The combined signals from the three solvents provide a recognition pattern for both metal ions at a certain concentration and realize the identification between Hg^{2+} and Cu^{2+}. Moreover, using principle component analysis, this method can be extended to identify metal ions that are hard to detect by the film sensor in water such as Co^{2+} and Ni^{2+}.

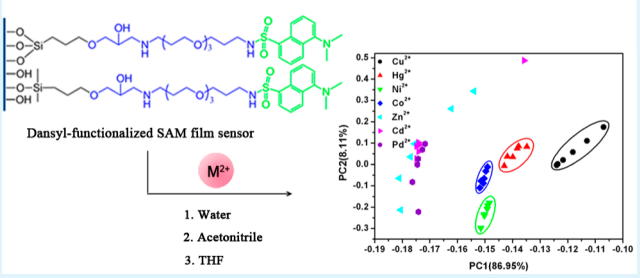

KEYWORDS: *metal ions, pattern recognition, sensor array, self-assembled monolayer, interface*

INTRODUCTION

Detecting and recognizing metal ions is of great interest to researchers because of the significant effect that metal ions have threw on our life.[1] On the one hand, a number of metal ions are essential trace elements closely related to human health, including zinc,[2] iron,[3] copper,[4] cobalt,[5] etc. A lack or excess of these trace elements that have certain physiology functions in the human body will cause a series of diseases. On the other hand, many heavy metal ions such as mercury,[6] lead,[7] and cadmium[8] are totally deleterious on human health.

Among various analytical methods for detecting metal ions, fluorescent chemical sensors composing a fluorophore for signal output and an ionophore for binding metal ions offer attractive advantages in terms of sensitivity, selectivity, and availability of multiple sensing parameters, which leads to various sensor design strategies.[9] Compared to numerous fluorescent molecular sensors for metal ions, fluorescent film sensors with fluorophores immobilized on solid surfaces provide additional merits such as reversibility and reproducibility which are crucial for practical applications and device implementation.[10−13] Self-assembled monolayers (SAMs) of organosilanes on SiO_2 surfaces afford an efficient way to generate stable and ordered fluorescent film sensors by chemically attaching fluorophores on the functional termini of SAMs.[14] The pioneer work of exploring the application of fluorescent SAM sensors for metal ions was conducted by Reinhoudt and co-workers.[15,16] They selected dansyl and coumarin as fluorescent probes and immobilized them on an amine-terminated SAM and found that the obtained fluorescent SAM sensors can be used for fluorescence sensing of metal ions without the need of selective receptor molecules.[16] Moreover, they also found that the connecting functionality of the fluorophore to the SAM monolayer is involved in the recognition process. This phenomenon was also observed by Fang et al., who have prepared a series of fluorescent SAM sensors for Cu^{2+} ions in aqueous solution by immobilizing polycyclic aromatic compounds (e.g., pyrene, dansyl, and anthracene) on epoxy-terminated SAMs.[17−20] They found that the fluorescent SAM films with polyamine in the spacer possessed higher sensitivity towards Cu^{2+} than those with diamine functionalities.[18,19] In addition, they also recovered that the polarity and flexibility of the spacer plays an important role in the sensing abilities of the obtained fluorescent SAM sensors.[21] Most of the reported fluorescent SAM sensors for Cu^{2+} by Fang et al. displayed high sensitivity only toward organic copper salts rather than inorganic ones due to the

Received: March 22, 2013
Accepted: December 13, 2013
Published: December 13, 2013

relatively hydrophobic spacers used in these film sensors.[17−20] Besides small PAHs as fluorescent probes, conjugated polymers were also used to prepare fluorescent SAM sensors for metal ions. For example, Lixiang Wang and co-workers reported to immobilize phosphonate-functionalized polyfluorene on amine-terminated SAM and realized a sensitive and selective film sensor for Fe^{3+} in aqueous solution.[22] Shu Wang et al. used amino-functionalized polyfluorene as fluorescent probe and developed a fluorescent SAM sensor for Cu^{2+} ions either in organic or inorganic salts.[23] However, fluorescent SAM sensors for metal ions are still limited and it is highly desirable to develop novel systems for different target metal ions.

Considering Hg^{2+} is highly toxic[24] and it can coordinate with N, O, and S atoms that possess lone pair electrons,[25] we developed a pyrene-modified fluorescent SAM sensor containing oligo(oxyethylene) and amino units in the spacer.[26] Although this film sensor displayed a high sensitivity for Hg^{2+} in aqueous solution as expected, it was also sensitive to the presence of Cu^{2+} either in organic or inorganic salts and unable to discriminate between Hg^{2+} and Cu^{2+}. To discriminate different metal ions, researchers have extensively used sensor arrays to provide distinct recognition pattern to each analyte by combining the signals from sensor elements that compose the array.[27,28] These sensor elements usually possess cross-reactive character, which is that all sensor elements respond differently towards an individual analyte and an individual sensor element responds differently towards all the tested analytes.[29] Reinhoudt et al. combined combinatorial approach and fluorescent SAMs to construct cross-reactive sensor arrays for identification of different series of metal ions.[30,31] However, this method relies on using various fluorophores in different sensor element to obtain cross-reactivity. As a consequence, such sensor arrays face disadvantages such as tedious preparation and data collecting process.

To realize the discrimination between Hg^{2+} and Cu^{2+} by a single fluorescent SAM sensor, a dansyl-functionalized fluorescent SAM sensor is particularly prepared in the present report using the spacer containing oligo(oxyethylene) and amino units. Dansyl is selected as the fluorescent probe due to its well-known microenvironment sensitivity[32] and exhibition of red-shift in fluorescence maximum emission with increased environmental polarity.[33] As previously reported, oligo(oxyethylene) and amine units in the spacer may ensure the sensitivity of the fluorescent SAM to Hg^{2+} and Cu^{2+}.[26] Thus, the dansyl-functionalized SAM sensor may display cross-reactive fluorescence responses to Hg^{2+} and Cu^{2+} in different solvents and provide recognition patterns for discriminating these two heavy metal ions.

EXPERIMENTAL SECTION

Reagents. 4,7,10-Trioxa-1,13-tridecanediamine (Sigma-Aldrich, 98%), dansyl chloride (Sigma-Aldrich, 98%), 3-glycidoxypropyltrimethoxysilane (GPTS; Acros, 97%) were used as received. $CuCl_2$, $HgCl_2$, $PbCl_2$, $ZnCl_2$, $CoCl_2$, and $CdCl_2$ are of analytical grade. Toluene is distilled from sodium under nitrogen prior to use. Trichloromethane ($CHCl_3$) is dried with anhydrous $CaCl_2$ overnight before use. Aqueous solutions of metal salts are prepared from Milli-Q water (18.2 MΩ cm at 25 °C). All other reagents are analytically pure. Glass substrates used for fabrication of SAM films are microscope slides with size of ~0.9 × 2.5 cm^2.

Methods. Fluorescence measurements were performed on a time-correlated single photon counting Edinburgh FLS 920 fluorescence spectrometer with a front-face method at room temperature. For a typical fluorescence titration assay, the fabricated film was first inserted into a cuvette containing 2.5 mL of testing solvent; the cuvette was then fixed on the solid sample holder with the film facing the excitation light source; after recording the original fluorescence emission of the film, a given volume of the stock aqueous solution of the tested metal ion was added under stirring; after this, the fluorescence emission of the film was recorded again in the presence of metal ions. The position of the film was kept constant during each set of measurement. Contact angles of the films were measured on a video-based contact angle measuring device SCA20. X-ray photoelectron spectroscopy (XPS) measurements were carried out on an ESCAPHI5400 photoelectron spectrometer. Atomic force microscopy (AFM) images were measured on a SOLVER P47 PRO system. ^{1}H NMR and ^{13}C NMR spectra were recorded on Bruker AV 400 NMR spectrometers. The high-resolution mass spectra (MS) were acquired in ESI positive mode using Bruker maxis UHR-TOF mass spectrometer. The FTIR spectra were obtained on a Fourier transform infrared spectrometer (Vertex 70v, Bruker, Germany).

Synthesis of N-(3-(2-(2-(3-Aminopropoxy)ethoxy)ethoxy)-propyl)-5-(dimethyl-amino)-naphthalene-1-sulfonamide (DNS-TOA). The diamine derivative of dansyl containing oligo(oxyethylene) as a linker, DNS-TOA, was synthesized by reacting dansyl chloride with the α,ω-diamine compound, 3,3′-((oxybis(ethane-2,1-diyl)) bis(oxy))-bis(propan-1-amine) (TOA). The synthesis procedure is as follows: A solution of dansyl chloride (150 mg, 0.56 mmol) in $CHCl_3$ (50 mL) was added dropwise to a solution of TOA (1.22 mL, 5.6 mmol) in $CHCl_3$ (50 mL) at 0 °C under stirring and N_2 atmosphere over a period of 8 h, after which the reaction system was stirred at room temperature for an extra hour. Then the mixture was washed with brine until the pH of the aqueous layer is neutral. The combined organic layer was acidified with 1 M HCl and then washed with $CHCl_3$. The separated aqueous layer was then basified (pH 9) with 3 M NaOH and extracted with $CHCl_3$. The organic layers were combined and dried over anhydrous $MgSO_4$, filtered, and concentrated in vacuo to afford yellowgreen oil DNS-TOA (210 mg, 83%). ^{1}H NMR (400 MHz, $CDCl_3$): δ 8.51 (d, J = 8.5 Hz, 1H, Ar H), 8.34 (d, J = 8.7 Hz, 1H, Ar H), 8.22 (d, J = 8.3 Hz, 1H, Ar H), 7.56−7.48 (m, 2H, Ar H), 7.17 (d, J = 7.5 Hz, 1H, Ar H), 3.64−3.41 (m, 12H, CH_2), 3.02 (d, J = 6.1 Hz, 2H, CH_2), 2.88 (s, 6H, CH_3), 2.84−2.80 (m, 2H, CH_2), 1.72−1.61 (m, 4H, CH_2), 1.25 (s, 2H, NH_2). ^{13}C NMR (101 MHz, $CDCl_3$): δ = 151.85 (C4, Ar C), 135.38 (C4, Ar C), 130.01 (C4, Ar C), 129.92 (CH, Ar C), 129.75 (CH, Ar C), 129.27 (CH, Ar C), 128.05 (C4, Ar C), 123.17 (CH, Ar C), 119.27 (CH, Ar C), 115.09 (CH, Ar C), 77.35 (CH_2), 77.03 (CH_2), 76.72 (CH_2), 70.50 (CH_2), 70.10 (CH_2), 69.45 (CH_2), 45.41 (CH_2), 41.51 (CH_3), 39.67 (CH_3), 32.46 (CH_2), 29.68 (CH_2), 28.95 (CH_2). FTIR (KBr plate, cm^{-1}): 3434 (−NH_2), 3290 (−NH), 3083 (Ar−H), 2922 (−CH_2), 1589 (Ar C═C), 1321 (−C−N), 1144 (O═S═O), 1094 (−C−O−C). HS-MS (ESI) $[M+H]^+$: calcd. for $C_{22}H_{36}N_3O_5S$, 454.2376; found, 454.2384. The ^{1}H NMR, ^{13}C NMR, MS, and IR spectra of DNS-TOA are provided in the Supporting Information (Figures S1−S4).

Preparation of DNS-TOA-Modified SAM Film (Film DNS-TOA). The originally ethanol-cleaned glass plate (S1) was treated in a freshly prepared "piranha solution" (7/3, V/V, 98%H_2SO_4/30%H_2O_2) (***warning**: piranha solution should be handled with extreme caution because it can react violently with organic matter*) for 1 h, and then rinsed thoroughly with plenty of water after the "piranha solution" cooled to room temperature, and dried with N_2 flow. The activated glass slide (S2) was immersed in the toluene solution of organosilane GPTS (0.6%, v/v, 50 mL) containing 20 μL of water for 12 h at 50 °C, to form epoxy-terminated SAM on the glass surface (S3). After this, the glass slide was rinsed with toluene and chloroform, successively, to remove any physisorbed GTPS.

The GPTS-covered glass slide was further macerated into the chloroform solution of DNS-TOA (6 mM) and then refluxed for 24 h. Dansyl moieties were expected to be chemically anchored to the glass surface via the surface reaction between epoxy termini and the amine groups of DNS-TOA. To remove unreacted DNS-TOA, the fabricated functionalized surfaces (S4) were rinsed thoroughly with chloroform, ethanol and water, successively. The fluorescence of the residue

Scheme 1. Synthesis Route of DNS-TOA and the Schematic Preparation of Dansyl-Functionalized SAM Film, Film DNS-TOA

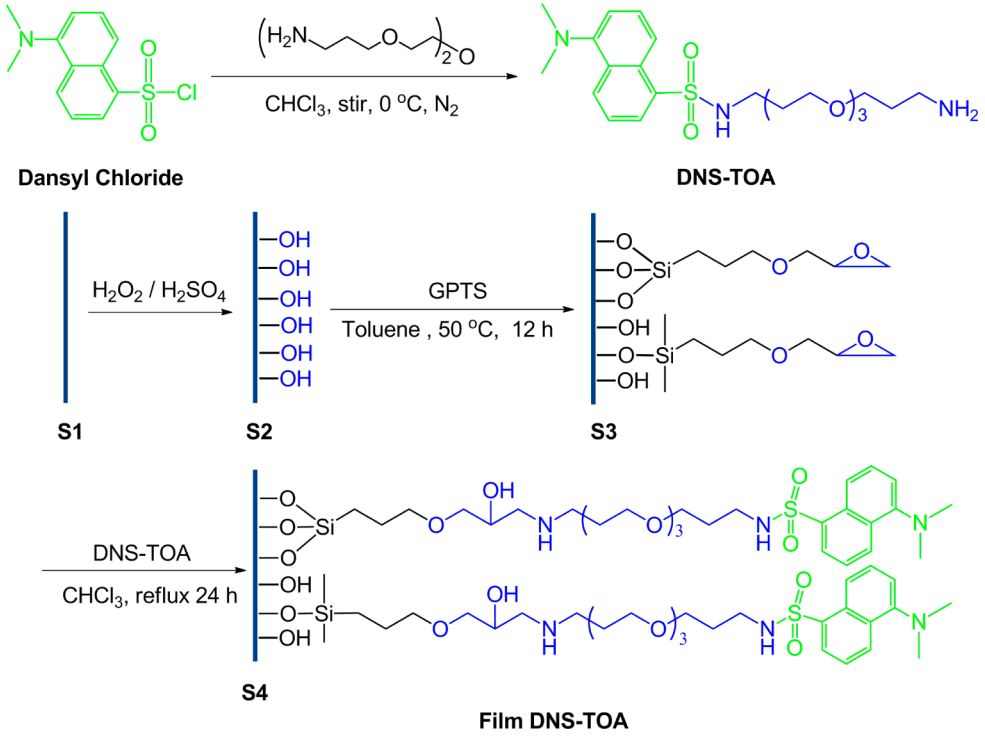

solvents for soaking Film DNS-TOA over 24 h was measured and no detectable fluorescence emission was found for the solvents (either water or organic solvents), suggesting that the leaking issue is negligible for the present film to function as a sensor. The synthesis of DNS-TOA and its coupling on the glass surface is schematically shown in Scheme 1.

RESULTS AND DISCUSSION

Surface Characterization of Film DNS-TOA. Three methods were employed to characterize the surfaces at different coupling stages. One is contact angle which has been extensively used to measure the wettability of SAM surfaces and provide information on polarity and chemical composition of the examined surfaces, one is XPS which could be used to offer information on the elemental composition of surface-supported organic adlayers,[34] and the third is AFM measurement for surface morphology.

The static contact angles (θ) with water for the surfaces at different coupling stage were measured at room temperature to monitor the surface variation. The results are presented in Figure 1. It can be seen that the activation with "piranha solution" reduces the contact angles of the glass slide significantly from 33.6 ± 0.1° to 5.6 ± 0.8°, indicating a large number of surface hydroxylic groups were generated after the activation process and increased the surface wettability. Further treatment with GPTS led to an increase of the contact angle to 44.7 ± 0.4°, suggesting reduction of surface hydrophilicity, which is in agreement with the formation of a silane adlayer on the surface. The coupling process with dansyl moieties generated a slight increase in the surface contact angle, which is 50.0 ± 0.3°. Though a long alkyl chain was introduced into the present film structure, the surface wettability was only slightly increased, which could be due to the hydrophilicity of tri-oxyethylene groups in the spacer. These results are in agreement with the expectation from the chemical compositions of the surfaces as shown in Scheme 1.

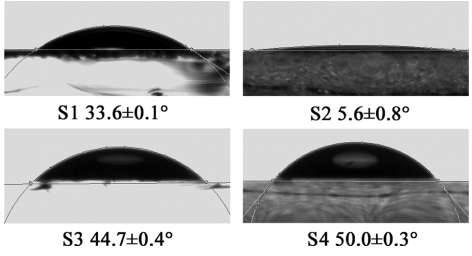

Figure 1. Images of static contact angles (θ) of various surfaces with water at r.t. S1, the original clean SiO_2 surface; S2, the "piranha solution" activated SiO_2 surface; S3, the silanized SiO_2 surface with epoxy-terminated SAM; S4, the dansyl-functionalized SiO_2 surface.

The XPS spectra of the glass slide surfaces were measured to evaluate the elemental compositions after each surface treatment. As depicted in Figure 2a, the C1s peak at 284.77 eV appears on S3, suggesting the formation of the organic silane adlayers on the surface after the silanization process. A further enhancement in C1s signal and appearance of N1s peaks at 400.96 eV were observed for S4, indicating the successful attachment of dansyl derivatives on the glass surface. The high-resolution XPS spectra in the C1s region were also examined to provide valuable information on the different oxidation states of surface carbon elements. Evidently, there are two different chemical binding states in C1s region for both S3 and S4 as seen from Figure 2b. One is at 284.23 eV assigned to aliphatic C−C and the other is at 285.63 eV assigned to C−O. Nevertheless, the ratio between these two chemical binding states is considerably different for these two surfaces. As for S3, there are 88.35 percent of C1s assigned to aliphatic C−C and only 11.65 percent assigned to C−O. However, in the dansyl-modified S4, the percentage for aliphatic C−C declines to 49.16% and the one for C−O ascends to 50.84%. The

dx.doi.org/10.1021/am405157k | ACS Appl. Mater. Interfaces 2014, 6, 49−56

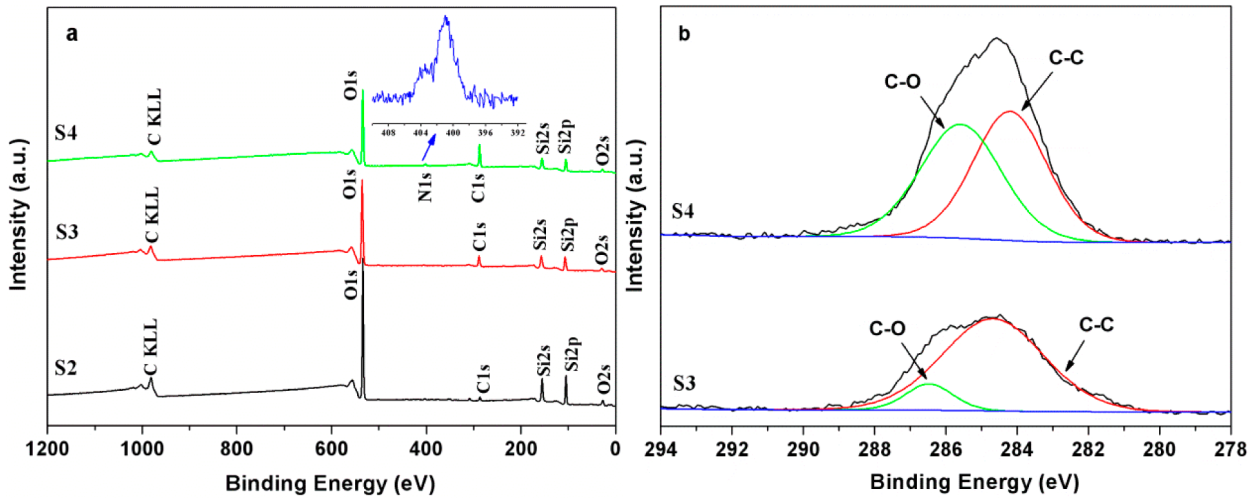

Figure 2. (a) XPS spectra and (b) high-resolution XPS spectra in C1s region for the surfaces at different coupling stage: (S2) the hydroxylated SiO_2 surface; (S3) the silanized SiO_2 surface with epoxy-termini; (S4) the DNS-TOA-functionalized SiO_2 surface.

significant increase in the ratio for C−O chemical binding states of C1s reveals the successful introduction of the oxyethylene units on the surface, confirming again the chemical coupling of the dansyl derivative on the surface.

AFM images of film DNS-TOA were also measured to check the morphologies of the dansyl-functionalized SAM film. As shown in Figure 3, the AFM image exhibits relatively uniform

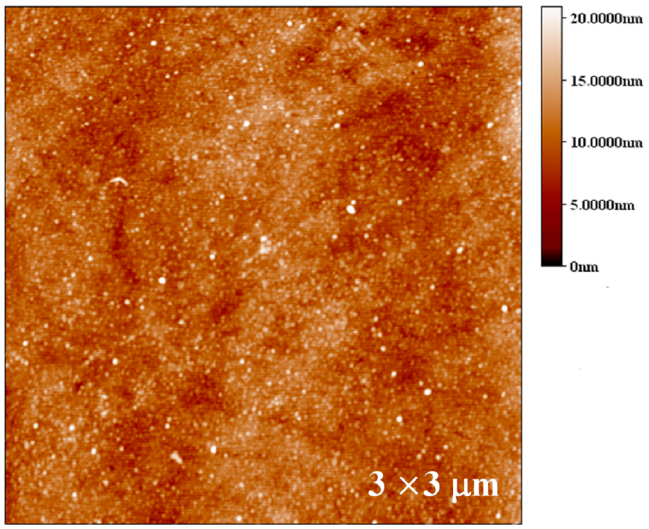

Figure 3. AFM image of the dansyl-functionalized SAM film (film DNS-TOA) on the surface of glass.

distribution of the fluorophore derivative on the surface. The height of immobilization area and that of blank substrate is determined to be ca. 12.84 ± 0.61 nm and 5.07 ± 0.5 nm, respectively, each of which is calculated from the average height of 18 different spots on the surface. Therefore, the thickness of the organic adlayer on the surface is ca. 7.77 nm. This is larger than the largest length of the corresponding monolayer as shown in Scheme 1 that is stimulated to be 4.53 nm. This is possibly due to the existence of multilayers on the surface formed by polymerization of trimethoxysilanes, which occurs easily in the presence of trace water as in our case.[35,36]

Photophysical Properties of Film DNS-TOA. To investigate the existence state of dansyl moieties on the surface, we recorded the steady-state fluorescence excitation and emission spectra of the film in water at different emission and excitation wavelengths. As shown in Figure 4a, the same profile and maximum wavelength of the fluorescence emission spectra are observed irrespective of the excitation wavelength and vice versa,[37] indicating that dansyl moieties exist in one uniform state on the substrate surface. The maximum excitation and maximum emission wavelengths are found at 350 and 515 nm and the emission and excitation bands have little superposition section, showing a large Stokes shift, and thereby the fluorophores in the immobilized state are not tending to be self-quenching.[11]

It is generally known that dansyl is commonly used as a polarity-sensitive probe because the position of its intramolecular charge transfer emission is sensitive to the polarity of its microenvironment.[38] Therefore, the emission spectra of film DNS-TOA in different solvents including water, THF, and acetonitrile were measured to examine if the polarity sensitivity was possibly conserved for the surface-bound dansyl moieties. THF and acetonitrile were selected because they are good solvents for DNS-TOA and have different polarity.[39] The spectra are illustrated in Figure 4b. It is found that the maximum emission appeared at 515, 512, and 506 nm in water, acetonitrile, and THF, respectively. Following the trend of solvent polarity decreasing from water to acetonitrile to THF,[39] the maximum emission of Film DNS-TOA is regularly blue shifted and the fluorescence intensity increases progressively. These results prove that the polarity sensitivity to the microenvironment was retained for the surface-bound dansyl moieties.[16] Thus, the different fluorescence behaviors including emission maximum and fluorescence intensity in the three pure solvents may endow the present film with cross-reactive responses to heavy metal ions.

Sensing Behaviors of Film DNS-TOA. In consideration of affinity of the tri-oxyethylene and amine units in the spacer to heavy metal ions,[40] the fluorescence responses of Film DNS-TOA to a series of metal ions at different concentration ranging from 0 to 10 μM in aqueous solution were first measured. The fluorescence intensity at 515 nm was recorded as I_0 and I in the absence and presence of metal ions, respectively. The fluorescence variation, I_0/I, upon each metal ion is illustrated in Figure 5. It can be seen that mercury and copper ions

dx.doi.org/10.1021/am405157k | ACS Appl. Mater. Interfaces 2014, 6, 49−56

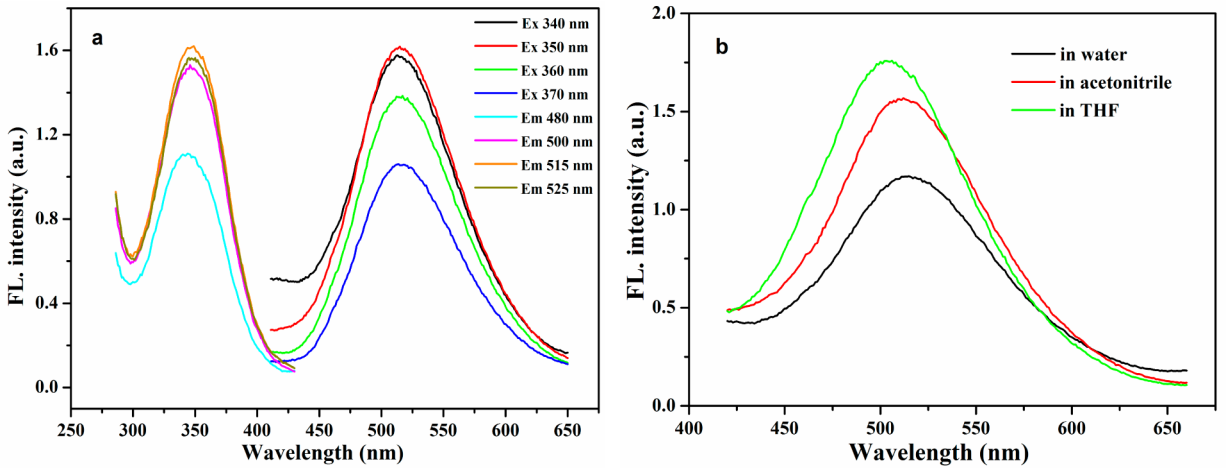

Figure 4. (a) Steady-state excitation and emission spectra of the Film DNS-TOA in water. (b) Fluorescence emission spectra of film DNS-TOA in different solvents (λ_{ex} =350 nm).

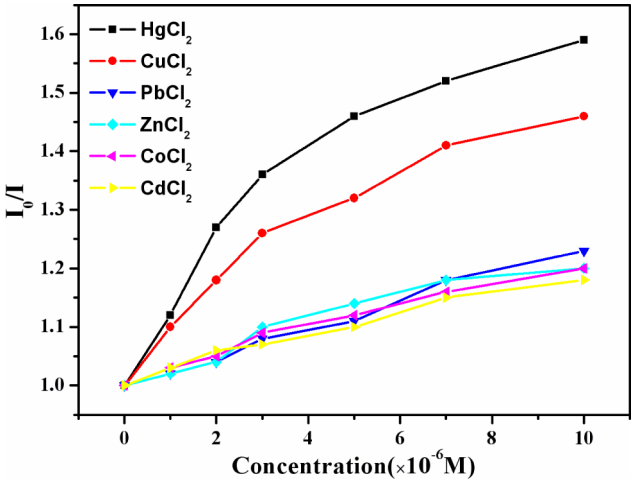

Figure 5. Fluorescence quenching plots of Film DNS-TOA by diverse metal ions in aqueous solution (measured at 515 nm).

produce higher fluorescence quenching than the other tested metal ions including Pb^{2+}, Zn^{2+}, Co^{2+}, and Cd^{2+}. This phenomenon declares that Film DNS-TOA is sensitive and selective to both mercury and copper ions. A similar result was observed in our previous work where a pyrene-functionalized SAM with the same spacer exhibits high sensitivity and selectivity toward both Hg^{2+} and Cu^{2+} in aqueous solution.[26] In that work, we attributed the sensitivity and selectivity to Hg^{2+} and Cu^{2+} of the pyrene-functionalized film sensor to the higher affinity of tri-oxyethylene and secondary amine units in the spacer to these two metal ions. However, direct evidence was not provided in that work. To check the binding ability, we measured UV−vis absorption of DNS-TOA in the presence of different metal ions. As seen in Figure S5 (see the Supporting Information), changes in the absorption spectrum of DNS-TOA in acetonitrile were only observed with the addition of Cu^{2+}. The absorption spectrum of DNS-TOA is characterized by a typical dansyl absorption at 338 nm,[41] which experiences a gradual blue shift to 302 nm and is accompanied with a new band emerging at 455 nm upon increasing addition of Cu^{2+}

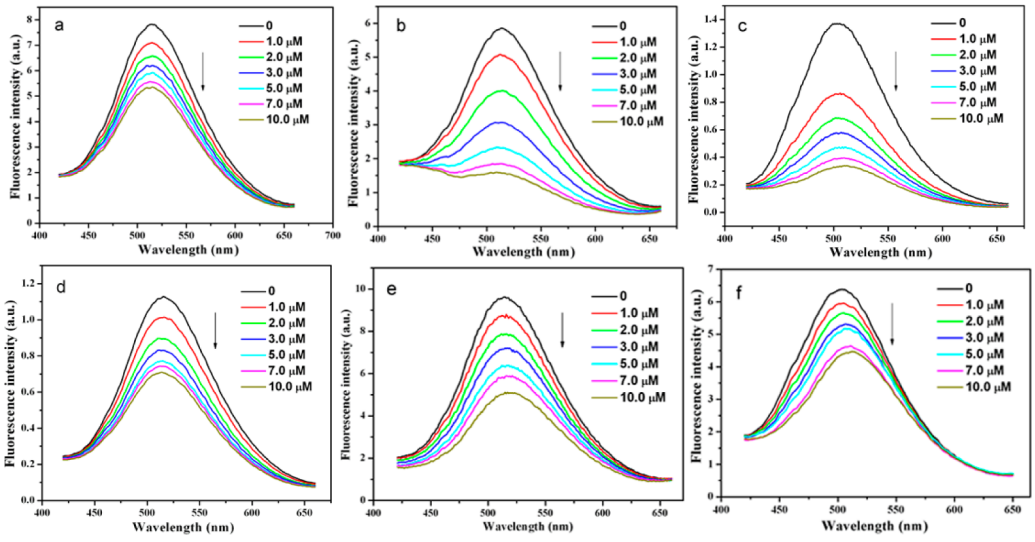

Figure 6. Fluorescence spectra of Film DNS-TOA upon the addition of Cu^{2+} in (a) water, (b) acetonitrile, and (c) THF, and Hg^{2+} in (d) water, (e) acetonitrile, and (f) THF (λ_{ex} = 350 nm).

dx.doi.org/10.1021/am405157k | ACS Appl. Mater. Interfaces 2014, 6, 49−56

(inset of Figure S5, see the Supporting Information). This indicates that copper ions form complexes with the fluorophores,[42] proving that Cu^{2+} has a higher affinity to DNS-TOA. The result also rules out the binding ability of DNS-TOA to mercury ions. The quenching effect of Hg^{2+} may come from the heavy atom effect.

However, the similar sensitivity makes the present film sensor hard to identify these two metal ions in aqueous solution. In view of the chemical attachment of the dansyl moieties on the glass surface and the reserved microenvironment-sensitivity, the film may feature cross-reactivity for responding these two metal ions in different solvents. If this is the case, the film may provide different response signals which compose a recognition pattern to each metal ion. Thus, a single film sensor can realize the identification of these two metal ions.

To verify this proof-of-concept, the fluorescence responses of Film DNS-TOA to mercury and copper ions were measured in water, acetonitrile and THF, respectively.[43] The obtained fluorescence emission spectra in different solvents upon metal ion concentration were displayed in Figure 6. It reveals that although the fluorescence intensity exhibits a general declining trend along metal ion concentration in all three solvents, the film illustrates a typical cross-reactive response to the two metal ions. On one hand, the reduction level of the fluorescence intensity of Film DNS-TOA toward the same metal ion (either Cu^{2+} or Hg^{2+}) is different in the three solvents. Take Cu^{2+} ion as an example, the fluorescence emission of the film decreases to 32% of its original intensity when 10 μM of Cu^{2+} is present in water (Figure 6a). When the solvent is shifted to acetonitrile and THF, the fluorescence reduction induced by 10 μM of Cu^{2+} is tremendously enhanced to 73 and 76%, respectively (Figure 6b, c). By comparison, the fluorescence quenching upon addition of 10 μM of Hg^{2+} in the three solvents are different from that observed for Cu^{2+}, where the highest quenching by Hg^{2+} is found in acetonitrile as it is 37% in water, 53% in acetonitrile, and 31% in THF, respectively (Figure 6d–f). On the other hand, the fluorescence responses of Film DNS-TOA to Cu^{2+} and Hg^{2+} are different in either solvent. For instance, in water, the film possesses a slight higher sensitivity toward Hg^{2+} than to Cu^{2+}. However, in both acetonitrile and THF, a much higher sensitivity is observed for Cu^{2+} than Hg^{2+}. The Stern–Volmer plots for Cu^{2+} and Hg^{2+} quenching Film DNS-TOA in the three solvents are provided in Figure S6 (see the Supporting Information). According to the Stern–Volmer equation, $I_0/I = 1 + K_{SV}[Q]$, the quenching constants (K_{SV}) by Cu^{2+} and Hg^{2+} in different solvents could be determined from the slopes of these Stern–Volmer plots. These K_{SV} values are calculated to be 3.9 ($\pm$0.5) $\times$ 10^4 M, 2.9 ($\pm$0.2) $\times$ 10^5 M, and 2.7 ($\pm$0.2) $\times$ 10^5 M for Cu^{2+} quenching Film DNS-TOA in water, acetonitrile, and THF, respectively; and are 4.8 ($\pm$0.1) $\times$ 10^4 M, 8.3 ($\pm$0.3) $\times$ 10^4 M, and 4.3 ($\pm$0.4) $\times$ 10^4 M, for Hg^{2+} quenching the film in the three corresponding solvents, respectively. The cross-reactive responses of Film DNS-TOA to Hg^{2+} and Cu^{2+} in the three solvents may enable it to provide pattern recognition of these two metal ions and identify them.

Therefore, the data of the fluorescence variation, I_0/I, upon the concentration of Cu^{2+} and Hg^{2+} in the three solvents were collected and displayed in Figure 7. I_0 and I stand for the maximum emission in the absence and presence of metal ions, respectively. As mentioned earlier, the maximum emission wavelength of Film DNS-TOA appeared at 515 nm in water, 512 nm in acetonitrile, and 506 nm in THF, respectively,

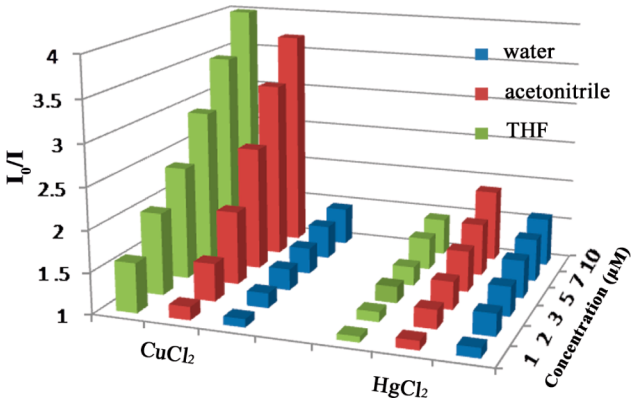

Figure 7. Quenching efficiencies of mercury and copper ions on the fluorescence emission of Film DNS-TOA in water, acetonitrile and THF, respectively (concentration ranging from 1 to 10 μM).

because of the polarity sensitivity of surface-confined dansyl moieties. Therefore, these three wavelengths were used for data acquisition. It is clearly seen that the responses of the film to Hg^{2+} in the three solvents is different from that to Cu^{2+}. The combined signals from the three solvents feature a characteristic pattern to each metal at a particular concentration. Interestingly, this phenomenon is analogous to a sensor array that generates a characteristic pattern (fingerprint) from all the sensor elements to distinguish the target analyte from each other. For this particular case, a single film plus different solvent function as a different sensor element to provide various fluorescence signals. Consequently, this single film sensor is capable of differentiating mercury ion and copper ion.

Because the fluorescence responses of the film sensor to Cu^{2+} and Hg^{2+} are remarkably varied when solvent is changed from water to acetonitrile and THF, this phenomenon may also occur to those other metal ions that induce slight fluorescence quenching in water. To check the possibility, the fluorescence variation of Film DNS-TOA to the other metal ions including Ni^{2+}, Zn^{2+}, Cd^{2+}, Co^{2+} and Pb^{2+} plus Hg^{2+} and Cu^{2+} were all measured at a fixed concentration of 2 μM in water, acetonitrile and THF, respectively. The bar chart of the variation in fluorescence intensity, I_0/I, at three selected wavelengths (515 nm in water, 512 nm in acetonitrile and 506 nm in THF) was collected and illustrated in Figure 8. Clearly, the fluorescence responses of Film DNS-TOA is various to the same metal ion in the three solvents. For example, the slight fluorescence quenching upon addition of Ni^{2+} and Co^{2+} in water was shifted to quite larger fluorescence quenching in THF and acetonitrile. For other metal ions like Zn^{2+}, Cd^{2+}, and Pb^{2+}, some increasing in quenching efficiency is also observed in the two organic solvents, but with a much lower extent. As a consequence, the fluorescence responses from Film DNS-TOA to these metal ions in the three solvents exhibit cross-reactive feature and generate a distinct pattern response (fingerprint) to each metal ion, as seen from the bar chart shown in Figure 8. Moreover, the responses of Film DNS-TOA to Cu^{2+} and Co^{2+} prepared in tap water were also monitored, where the tap water sample of Cu^{2+} and Co^{2+} was added to the testing solvent (pure water, acetonitrile, or THF) containing the film. It is found that although the film exhibits lower sensitivity to the tap water samples in all cases, the cross-reactive responses to these metal ions were observed (see Figure S7 in the Supporting Information), indicating the potentials of using the present film for real sample detection.

dx.doi.org/10.1021/am405157k | ACS Appl. Mater. Interfaces 2014, 6, 49–56

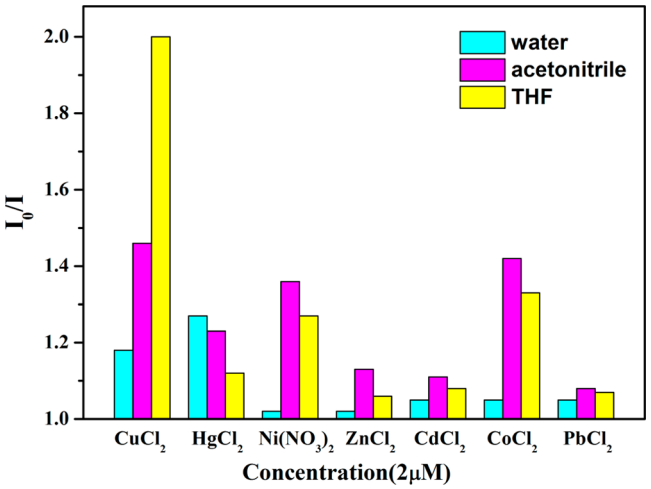

Figure 8. Recognition patterns for metal ions (concentration at 2 μM) by collecting fluorescence quenching data in three different solvents at the maximum wavelengths ($\lambda_{em,max}$(water) = 515 nm; $\lambda_{em,max}$(acetonitrile) = 512 nm; $\lambda_{em,max}$(THF) = 506 nm).

To check the identification ability of the film to these metal ions, we conducted further experiments for measuring the fluorescence quenching induced by these other metal ions in the three solvents over a concentration range from 1 to 10 μM, and primary component analysis (PCA) were used to analyze the obtained data. PCA is a nonsupervised method used to reduce the dimensionality of a data set in order to make it easier to interpret.[44,45] This is accomplished by calculating orthogonal eigenvectors (principal components, PC) that lie in the direction of the maximum variance within that data set. Usually, the highest degree of variance is provided by the first PC, and other PCs follow in the order of decreasing variance. As a result, the PCA concentrates the most significant characteristics (variance) of the data into a lower dimensional space. The resulting two-dimensional PCA score plot is illustrated in Figure 9. As observed, the first principle component (PC1) carries ca. 86.9% of the variance while the second principle component (PC2) carries ca. 8.1%. Altogether these two components carry about 95% of the whole variance

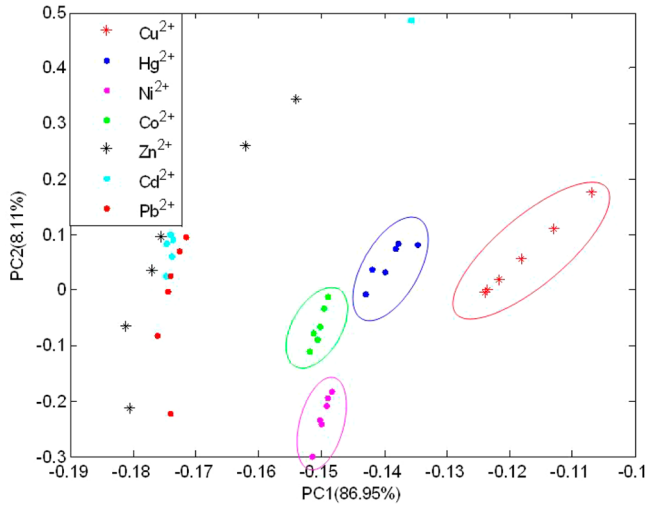

Figure 9. Two-dimensional PCA score plot for discrimination of metal ions at different concentrations (1, 2, 3, 5, 7, and 10 μM).

in the data. According to these PCA data, the film sensor can not only identify Cu^{2+} and Hg^{2+}, but also recognize Ni^{2+} and Co^{2+} that are hardly detectable when only measured in water. However, the low quenching efficiencies of Pb^{2+}, Zn^{2+} and Cd^{2+} in the three solvents make it is hard to discriminate among these three metal ions. Even so, these results are still quite significant since one single film sensor is able to identify four different heavy metal ions by only varying detecting solvents, which is usually achieved by a sensor array composing of different sensor elements.

CONCLUSION

A dansyl-functionalized SAM film sensor via a spacer containing metal-ion binding units, oligo(oxyethylene) groups, was specially designed, prepared, and characterized by contact angle measurements, XPS, and fluorescence techniques. Studies from solvent effect revealed that the polarity-sensitivity was retained for the surface-confined dansyl moieties, where the emission maximum gradually blue-shifts from 515 nm in water to 512 nm in acetonitrile and 506 nm in THF. Fluorescence quenching studies declare that the higher sensitivity towards Hg^{2+} and Cu^{2+} over the other tested divalent metal ions including Zn^{2+}, Cd^{2+}, Co^{2+}, and Pb^{2+} was preserved for the dansyl-functionalized film sensor. Attractively, further measurements of the fluorescence responses of the film towards Cu^{2+} and Hg^{2+} in three solvents including water, acetonitrile, and THF reveal that the present film exhibits analogous cross-reactive responses to these two metal ions. The fluorescence quenching extent is not only different in the three solvents for a particular metal ion, but also different to the two metal ions in a particular solvent. As a consequence, the combined fluorescence quenching signals obtained from the three solvents generate a distinct recognition pattern for the two metal ions at a particular concentration and realize the discrimination between Hg^{2+} and Cu^{2+}. Moreover, principle component analysis find that this film can also identify those metal ions that are hardly detectable when only measured in water such as Co^{2+} and Ni^{2+}.

The proof-of-principle experiments conducted in the present work demonstrate that using a single film sensor functionalized with microenvironment-sensitive fluorophore to provide cross-reactive responses in different solvents can realize pattern recognition of different metal ion targets. This strategy remarkably simplifies the process of preparation and data collection for using fluorescent sensor arrays.

ASSOCIATED CONTENT

Supporting Information

^{1}H NMR, ^{13}C NMR, MS, IR spectra of DNS-TOA, UV−vis absorption spectra of DNS-TOA in the presence of metal ions, Stern−Volmer plots of metal ions quenching Film DNS-TOA, and pattern recognition of metal ions in tap water. This material is available free of charge via the Internet at http://pubs.acs.org.

AUTHOR INFORMATION

Corresponding Authors

*E-mail: dinglp33@snnu.edu.cn. Phone/Fax: +86-29-81530789, +86-29-81530727.
*E-mail: yfang@snnu.edu.cn. Phone/Fax: +86-29-85310081, +86-29-85310079.

Notes

The authors declare no competing financial interest.

■ ACKNOWLEDGMENTS

The authors acknowledge the financial support from National Natural Science Foundation of China (21173142, 20927001), Shaanxi Provincial Department of Science and Technology (2010K01-112, 2011KJXX48), Program for "Changjiang Scholars and Innovative Research Team in University" (IRT1070), and the Fundamental Research Funds for the Central Universities (GK201301006). We also thank Dr. Yunhong Xin for the help with PCA data handling.

■ REFERENCES

(1) Valeur, B.; Leray, I. *Coord. Chem. Rev.* **2000**, *205*, 3−40.
(2) Nguyen, D. M.; Frazer, A.; Rodriguez, L.; Belfield, K. D. *Chem. Mater.* **2010**, *22*, 3472−3481.
(3) Saikia, G.; Iyer, P. K. *Macromolecules* **2011**, *44*, 3753−3758.
(4) Martínez, R.; Espinosa, A.; Tárraga, A.; Molina, P. *Tetrahedron* **2010**, *66*, 3662−3667.
(5) Lee, J. H.; Jeong, A. R.; Shin, I.-S.; Kim, H.-J.; Hong, J.-I. *Org. Lett.* **2010**, *12*, 764−767.
(6) Zhao, Q.; Cao, T.; Li, F.; Li, X.; Jing, H.; Yi, T.; Huang, C. *Organometallics* **2007**, *26*, 2077−2081.
(7) Xia, W.-S.; Schmehl, R. H.; Li, C.-J.; Mague, J. T.; Luo, C.-P.; Guldi, D. M. *J. Phys. Chem. B* **2002**, *106*, 833−843.
(8) Varriale, A.; Staiano, M.; Rossi, M.; D'Auria, S. *Anal. Chem.* **2007**, *79*, 5760−5762.
(9) Liu, Z.; He, W.; Guo, Z. *Chem. Soc. Rev.* **2013**, *42*, 1568−1600.
(10) Zheng, Y.; Gattás-Asfura, K. M.; Li, C.; Andreopoulos, F. M.; Pham, S. M.; Leblanc, R. M. *J. Phys. Chem. B* **2003**, *107*, 483−488.
(11) Zheng, Y.; Orbulescu, J.; Ji, X.; Andreopoulos, F. M.; Pham, S. M.; Leblanc, R. M. *J. Am. Chem. Soc.* **2003**, *125*, 2680−2686.
(12) Jin, P.; Chu, J.; Miao, Y.; Tan, J.; Zhang, S.; Zhu, W. *AIChE J.* **2013**, *59*, 2743−2752.
(13) Jin, P.; Guo, Z.; Chu, J.; Tan, J.; Zhang, S.; Zhu, W. *Ind. Eng. Chem. Res.* **2013**, *52*, 3980−3987.
(14) Flink, S.; van Veggel, F. C. J. M.; Reinhoudt, D. N. *J. Phys. Org. Chem.* **2001**, *14*, 407−415.
(15) van der Veen, N. J.; Flink, S.; Deij, M. A.; Egberink, R. J. M.; van Veggel, F. C. J. M.; Reinhoudt, D. N. *J. Am. Chem. Soc.* **2000**, *122*, 6112−6113.
(16) Crego-Calama, M.; Reinhoudt, D. N. *Adv. Mater.* **2001**, *13*, 1171−1174.
(17) Lü, F.; Gao, L.; Ding, L.; Jiang, L.; Fang, Y. *Langmuir* **2006**, *22*, 841−845.
(18) Ding, L.; Cui, X. a.; Han, Y.; Lü, F.; Fang, Y. *J. Photochem. Photobiol., A* **2007**, *186*, 143−150.
(19) Hu, J.; Lü, F.; Ding, L.; Zhang, S.; Fang, Y. *J. Photochem. Photobiol., A* **2007**, *188*, 351−357.
(20) Lü, F.; Gao, L.; Li, H.; Ding, L.; Fang, Y. *Appl. Surf. Sci.* **2007**, *253*, 4123−4131.
(21) Du, H.; He, G.; Liu, T.; Ding, L.; Fang, Y. *J. Photochem. Photobiol., A* **2011**, *217*, 356−362.
(22) Wu, X.; Xu, B.; Tong, H.; Wang, L. *Macromolecules* **2010**, *43*, 8917−8923.
(23) Lv, F.; Feng, X.; Tang, H.; Liu, L.; Yang, Q.; Wang, S. *Adv. Funct. Mater.* **2011**, *21*, 845−850.
(24) Metivier, R.; Leray, I.; Lebeau, B.; Valeur, B. *J. Mater. Chem.* **2005**, *15*, 2965−2973.
(25) Nolan, E. M.; Lippard, S. J. *Chem. Rev.* **2008**, *108*, 3443−3480.
(26) Cao, Y.; Ding, L.; Hu, W.; Wang, L.; Fang, Y. *Appl. Surf. Sci.* **2013**, *273*, 542−548.
(27) Palacios, M. A.; Wang, Z.; Montes, V. A.; Zyryanov, G. V.; Anzenbacher, P. *J. Am. Chem. Soc.* **2008**, *130*, 10307−10314.
(28) Palacios, M. A.; Wang, Z.; Montes, V. A.; Zyryanov, G. V.; Hausch, B. J.; Jursikova, K.; Anzenbacher, P., Jr *Chem. Commun.* **2007**, 3708−3710.
(29) Anzenbacher, J. P.; Lubal, P.; Bucek, P.; Palacios, M. A.; Kozelkova, M. E. *Chem. Soc. Rev.* **2010**, *39*, 3954−3979.
(30) Basabe-Desmonts, L.; Beld, J.; Zimmerman, R. S.; Hernando, J.; Mela, P.; García Parajó, M. F.; van Hulst, N. F.; van den Berg, A.; Reinhoudt, D. N.; Crego-Calama, M. *J. Am. Chem. Soc.* **2004**, *126*, 7293−7299.
(31) Basabe-Desmonts, L.; Van der Baan, F.; Zimmerman, R.; Reinhoudt, D.; Crego-Calama, M. *Sensors* **2007**, *7*, 1731−1746.
(32) Grieser, F.; Thistlethwaite, P.; Urquhart, R.; Patterson, L. K. *J. Phys. Chem.* **1987**, *91*, 5286−5291.
(33) Ghiggino, K. P.; Lee, A. G.; Meech, S. R.; Connor, D. V. O.; Phillips, D. *Biochemistry* **1981**, *20*, 5381−5389.
(34) Flink, S.; van Veggel, F. C. J. M.; Reinhoudt, D. N. *Adv. Mater.* **2000**, *12*, 1315−1328.
(35) Ofir, Y.; Zenou, N.; Goykhman, I.; Yitzchaik, S. *J. Phys. Chem. B* **2006**, *110*, 8002−8009.
(36) Ito, Y.; Virkar, A. A.; Mannsfeld, S.; Oh, J. H.; Toney, M.; Locklin, J.; Bao, Z. *J. Am. Chem. Soc.* **2009**, *131*, 9396−9404.
(37) Lakowicz, J. R. In *Principles of Fluorescence Spectroscopy*, 2nd ed.; Kluwer Academic/Plenum Publisher: New York, 1999; Vol. *1*, p 7.
(38) Page, P. M.; Munson, C. A.; Bright, F. V. *Langmuir* **2004**, *20*, 10507−10516.
(39) Reichardt, C. *Chem. Rev.* **1994**, *94*, 2319−2358.
(40) Manandhar, E.; Wallace, K. J. *Inorg. Chim. Acta* **2012**, *381*, 15−43.
(41) Dhir, A.; Bhalla, V.; Kumar, M. *Org. Lett.* **2008**, *10*, 4891−4894.
(42) Kaur, K.; Kumar, S. *Dalton Trans.* **2011**, *40*, 2451−2458.
(43) Note: The fluorescence spectra of Film DNS-TOA in solvent mixtures (e.g. acetonitrile:water and THF:water) were also measured. However, much smaller shifts were observed in mixtures compared to that in pure organic solvent. Thus, the sensing behaviors of Film DNS-TOA in mixed solvents were not examined.
(44) Ding, L.; Liu, Y.; Cao, Y.; Wang, L.; Xin, Y.; Fang, Y. *J. Mater. Chem.* **2012**, *22*, 11574−11582.
(45) Palacios, M. A.; Nishiyabu, R.; Marquez, M.; Anzenbacher, P., Jr. *J. Am. Chem. Soc.* **2007**, *129*, 7538−7544.